Stoichiometry of the degradation of dissolved and particulate biogenic organic matter in the NW Iberian upwelling

X. A. Álvarez-Salgado,[1] M. Nieto-Cid,[1] J. Gago,[1] S. Brea,[1] C. G. Castro,[1] M. D. Doval,[2] and F. F. Pérez[1]

Received 7 May 2004; revised 27 February 2006; accepted 13 March 2006; published 20 July 2006.

[1] The average composition of the dissolved and particulate products of early degradation of marine phytoplankton has been established for the first time in a coastal upwelling system using a mixing analysis along isopycnal surfaces combined with a stoichiometric model. About 17–18% of the mineralized organic matter is derived from the decomposition of organic particulates, and 16–35% is from the dissolved organic matter. The remaining 50–70% is derived probably from large fast sinking particles. On average, the mineralized material on large particles has the closest composition to the Redfield formula. The ratio of dissolved saccharides to dissolved organic matter respiration is >40% higher than expected from a material of Redfield composition. Finally, the ratio of lipid to particulate organic matter respiration is >80% larger than expected from a material of Redfield composition. Regarding the decomposition of hard structures, biogenic silica dissolves predominantly in the inner shelf, where organic carbon oxidation is more intense, and diatom deposition occurs preferentially.

Citation: Álvarez-Salgado, X. A., M. Nieto-Cid, J. Gago, S. Brea, C. G. Castro, M. D. Doval, and F. F. Pérez (2006), Stoichiometry of the degradation of dissolved and particulate biogenic organic matter in the NW Iberian upwelling, *J. Geophys. Res.*, *111*, C07017, doi:10.1029/2004JC002473.

1. Introduction

[2] The composition of the products of early degradation of phytoplankton photosynthesis has been a matter of controversy over the last 50 years, after the seminal study of *Redfield et al.* [1963]. On the basis of that work, *Richards* [1965] established an average composition of $C_{106}H_{264}O_{110}N_{16}P$. Subsequently, *Anderson* [1995] and *Fraga et al.* [1998] proposed revised formulas, $C_{106}H_{175}O_{42}N_{16}P$ and $C_{106}H_{171}O_{42}N_{16}P$ respectively, which basically corrected the overestimated H and O proportions of the original *Richard's* [1965] formula.

[3] Some authors have asserted that the respiration ratios of biogenic organic matter, $-O_2$/C/N/P, in the ocean interior are invariant with depth and basin [e.g., *Takahashi et al.*, 1985; *Anderson and Sarmiento*, 1994]. Others considered that there is a fractionation during the decomposition of biogenic organic matter, in such a way that the most labile P- and N-rich materials are oxidized preferentially at shallower depths [e.g., *Martin et al.*, 1987; *Minster and Boulahdid*, 1987; *Shaffer et al.*, 1999; *Brea et al.*, 2004] or in more ventilated ocean basins [*Li and Peng*, 2002]. Modifications in the quality and quantity of the sinking materials exported from the upper ocean [*Pahlow and Riebesell*, 2000] and changes in source water type properties [*Gruber et al.*, 2000] have also been argued to explain these inter basin differences.

[4] Another matter of open discussion is the relative contribution of dissolved, suspended and sinking organic matter to oxygen consumption in the oceans. Some authors maintain that the oxidation of large, fast sinking particles has to be the dominant process to keep the apparent constancy of the $-O_2$/C/N/P ratios [*Anderson and Sarmiento*, 1994]. On the contrary, others propose fractionation during the respiration of suspended organic matter [*Copín-Montegut and Copín-Montegut*, 1983; *Garber*, 1984; *Martin et al.*, 1987; *Sambrotto et al.*, 1993; *Schneider et al.*, 2003]. The model of *Suess and Müller* [1980] incorporates strong elemental fractionation of particulate organic matter (POM) through the water column by preferential removal of N- and P-containing organic compounds. Considering that dissolved organic matter (DOM) may constitute as much as 30% of the flux of biogenic materials transported to the deep ocean [*Yamanaka and Tajika*, 1997], and that DOM appears to have higher C/N/P ratios than POM [e.g., *Clark et al.*, 1998; *Loh and Bauer*, 2000; *Hopkinson et al.*, 1997, 2002], its role in the marine carbon/nutrient cycle cannot be ignored.

[5] Biogenic matter production is enhanced in the coastal zone because of intensified nutrient fluxes from the ocean, the continents and the atmosphere [*Walsh*, 1991]. Average primary production per unit area in the coastal zone, 250 g C m^{-2} yr^{-1}, is more than twice that in the open

[1]Instituto de Investigacións Mariñas, Consejo Superior de Investigaciones Científicas, Vigo, Spain.
[2]Xunta de Galicia, Instituto Tecnolóxico de Medio Mariño (INTECMAR), Vilagarcía de Arousa, Spain.

0148-0227/06/2004JC002473

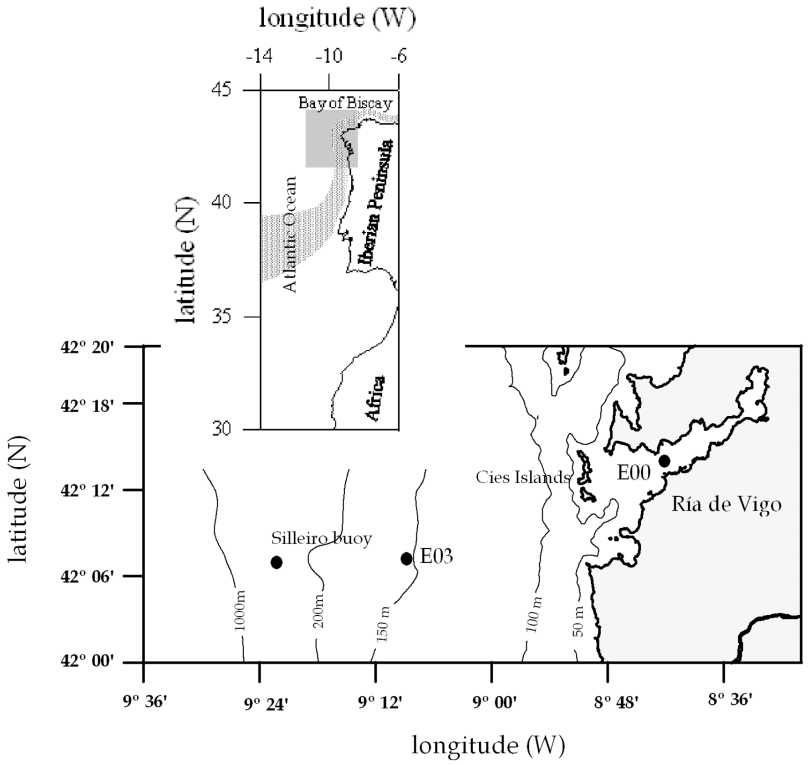

Figure 1. Map of the study area, the Ría de Vigo and adjacent open shelf waters. The positions of the sampling stations in the middle ría (station 00) and the middle shelf (station 03), as well as the Silleiro SeaWatch buoy meteorological observatory, are indicated. The isobaths of −50, −100, −150, −200, and −1000 m are also depicted. The Iberian poleward current (IPC) is depicted in the inset.

ocean, 90 g C m^{-2} yr^{-1} [*Wollast*, 1998]. As a result, the decomposition of biogenic materials is also enhanced. About 83% of the ocean benthic respiration and 87% of the burial occurs in the sediments of the coastal zone [*Middelburg et al.*, 1993]. Pelagic and benthic degradation processes are specially intensified in coastal upwelling areas, because of the magnified entry of nutrients.

[6] The aim of this work is to study the elemental and biochemical compositions of (1) the organic matter dissolved in seawater, (2) soft and hard particulates suspended in water and (3) biogenic materials that have been mineralized in the water column of the NW Iberian upwelling system. Our investigation was conducted in two contrasting environments: the system of large, V-shaped embayments of Galicia (NW Spain), known as Rías Baixas (Figure 1) and the adjacent open shelf. Although the rías are singular ecosystems, their large dimensions and their well-known hydrodynamic and biogeochemical behavior make them similar to any coastal upwelling system at comparable latitudes: off Oregon (NW America) or off Chile (SW America).

2. Study Area

[7] This study is focused on the NW Iberian upwelling system (42°−43°N), at the boundary between the temperate and subpolar regimes of the eastern North Atlantic (Figure 1). Wind stress/relaxation cycles of period 1−2 week take place from March−April to September−October, the upwelling season [*Álvarez-Salgado et al.*, 1993]. Downwelling prevails the rest of the year, favoring a reversal of the coastal circulation with the arrival of warm and salty subtropical surface and central waters to our latitudes in the form of the well-defined slope Iberian Poleward Current (IPC) [*Álvarez-Salgado et al.*, 2003]. The winter mixing period occurs at the time of the transition from the downwelling to the upwelling seasons.

[8] Two contrasting environments were sampled: (1) the Ría de Vigo, a 2.5 km^3 large V-shaped embayment, which is primarily controlled by coastal winds and secondarily by continental runoff [*Gilcoto et al.*, 2001]; and (2) the adjacent shelf, which exchanges water and materials with the rías and the open ocean and is affected by strong alongshore currents. Both environments are connected during the upwelling season, when the surface waters of the ría are exported to the adjacent shelf and the bottom waters of the shelf enters the ría. On the contrary, during the downwelling season a convergence front develops between the subtropical IPC waters transported onshore by the Ekman transport and the waters of the ría transported offshore by the continental runoff [*Álvarez-Salgado et al.*, 2000].

3. Sampling and Analytical Methods

3.1. Sampling Strategy

[9] Two stations were sampled weekly from May 2001 to April 2002: station 00 was in the middle segment of the Ría de Vigo (45 m depth) and station 03 was in the middle shelf (150 m depth). Samples were taken with a rosette sampler equipped with twelve 10-L PVC Niskin bottles with

stainless-steel internal springs. Salinity and temperature were recorded with a SBE 9/11 conductivity-temperature-depth probe attached to the rosette sampler. Conductivity measurements were converted into practical salinity scale values with the equation of *UNESCO* [1986].

[10] Samples for the analyses of dissolved oxygen, pH, total alkalinity, nutrient salts, dissolved and particulate organic carbon and nitrogen were collected from 5, 15 and 40 m at station 00 and 5, 25, 40, 60, 75, 100 and 150 m at station 03 with a weekly periodicity. Samples for dissolved and particulate organic phosphorus and saccharides were taken at the same depths but with a fortnightly periodicity.

3.2. Nutrient Salts (NH_4^+, NO_2^-, NO_3^-, HPO_4^{2-}, and SiO_4H_4)

[11] Water samples were collected in 50-mL polyethylene bottles; they were kept cold (4°C) until analysis in the laboratory using standard segmented flow analysis (SFA) procedures. The precisions are ±0.02 μM for nitrite, ±0.1 μM for nitrate, ±0.05 μM for ammonium, ±0.02 μM for phosphate and ±0.05 μM for silicate.

3.3. Dissolved Oxygen (O_2)

[12] It was directly collected into calibrated 110 mL glass flasks and, after fixation; they were kept in the dark until analysis in the laboratory 24 h later. O_2 was determined by Winkler potentiometric endpoint titration using a Titrino 720 analyzer (Metrohm) with a precision of ±0.5 μmol kg^{-1}. The apparent oxygen utilization, AOU = O_2sat − O_2, was calculated using the algorithm proposed by Benson & Krause [*UNESCO*, 1986] for oxygen saturation (O_2sat).

[13] The corrected dissolved oxygen (O_{2C}) is the O_2 concentration in the water column when all the inorganic nitrogen is in the oxidation state of nitrate. Since 0.5 mole of oxygen are necessary to oxidize 1 mole of nitrite to nitrate and 2 moles of oxygen are required to oxidize 1 mole of ammonium to nitrate, O_{2C} is calculated as [*Ríos et al.*, 1989]

$$O_{2C} = O_2 - 0.5 \times NO_2^- - 2 \times NH_4^+ \quad (1)$$

3.4. Total Alkalinity (TA) and Total Inorganic Carbon (C_T)

[14] Samples for TA and pH (total hydrogen concentration scale, 25°C) were collected into 500-mL glass flasks and analyzed within a few hours in the base laboratory. Seawater pH was measured spectrophotometrically following *Clayton and Byrne* [1993]. The precision is ±0.003 pH units. TA was determined by titration to pH 4.4 with HCl, according to the potentiometric method of *Pérez and Fraga* [1987] with a precision of ±2 μmol kg^{-1}. The potential alkalinity (TA_P) was calculated following *Fraga and Álvarez-Salgado* [2005]:

$$TA_P = TA - NH_4^- + 0.93 \times NO_2^- + NO_3^- + 0.08 \times \left(NH_4^+ + NO_2^- + NO_3^-\right) + 0.23 \times HPO_4^{2-} \quad (2)$$

[15] Total inorganic carbon (C_T) was calculated from pH and TA with the carbonic and boric acid dissociation constants of *Lueker et al.* [2000]. The estimated precision of this calculation is ±3 μmol kg^{-1}.

[16] The influence of the precipitation/dissolution of $CaCO_3$ on C_T can be corrected by subtracting ½ of TA_P to C_T [*Broecker and Peng*, 1982]. The resulting variable is called corrected C_T (C_{TC}):

$$C_{TC} = C_T - \frac{1}{2} \times TA_P \quad (3)$$

3.5. Dissolved Organic Carbon (DOC) and Nitrogen (DON)

[17] Samples were taken into 500-mL acid-cleaned flasks and filtered through precombusted (450°C, 4 hours) 47 mm diameter Whatman GF/F filters (nominal pore size, 0.7 μm) in an acid-cleaned glass filtration system, under low N_2 flow pressure. Aliquots for the analysis of DOC/DON were collected into 10 mL precombusted (450°C, 12 hours) glass ampoules. After acidification with H_3PO_4 to pH < 2, the ampoules were heat-sealed and stored in the dark at 4°C until analysis. DOC and DON were measured simultaneously with a nitrogen-specific Antek 7020 nitric oxide chemiluminescence detector, coupled in series with the carbon-specific Infrared Gas Analyzer of a Shimadzu TOC-5000 organic carbon analyzer [*Álvarez-Salgado and Miller*, 1998]. The precision is ±0.7 μmol C L^{-1} for carbon and ±0.2 μmol N L^{-1} for nitrogen. Their respective accuracies were tested daily with the reference materials provided by Prof. D. Hansell (Univ. of Miami). We obtained an average concentration of 45.7 ± 1.6 μmol C L^{-1} and 21.3 ± 0.7 μmol N L^{-1} (n = 26) for the deep ocean reference (Sargasso Sea deep water, 2600 m) minus blank reference materials. The nominal value for TOC provided by the reference laboratory is 44.0 ± 1.5 μmol C L^{-1}; a consensus total dissolved nitrogen (TDN) value has not been supplied yet, but a mean ± SD value of 22.1 ± 0.8 μmol N L^{-1} for four HTCO systems and 21.4 μmol N L^{-1} for one persulphate oxidation method has been provided by *Sharp et al.* [2004] as a result of the Lewes intercalibration exercise. DON was obtained by subtracting N_T (=ammonium + nitrite + nitrate) from TDN.

3.6. Dissolved Organic Phosphorus (DOP)

[18] Samples were taken and filtered as indicated for DOC/DON. The filtrate was collected into 50 mL polyethylene containers and frozen at −20°C until analysis. It was measured by the SFA system for phosphate, after oxidation with $Na_2S_2O_8$/borax and UV radiation [*Armstrong et al.*, 1966]. Only the organic mono-phosphoric esters are analyzed because poly-phosphates are resistant to this oxidation procedure. Daily calibrations with phosphate, phenyl phosphate and adenosine 5′-monophosphate (AMP) in seawater were carried out. Standards of AMP were determined in order to calculate the mono-phosphoric esters recovery (∼80%). The precision of the method is ±0.04 μmol P L^{-1}.

3.7. Dissolved Monosaccharides and Total Saccharides

[19] Sampling and storage procedures are identical to for DOP samples. Mono and total saccharides were determined by the oxidation of the free reduced sugars with 2,4,6-

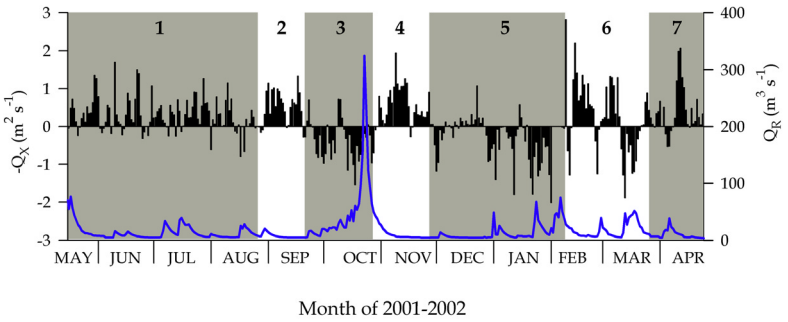

Figure 2. Seasonal evolution of the offshore Ekman transport ($-Q_X$) calculated with wind data provided by the Silleiro SeaWatch buoy (http://www.puertos.es/index.jsp). The freshwater discharge to the Ría the Vigo (Q_R) is also shown. $-Q_X$, bars; Q_R, solid line.

tripyridyl-s-triazine (TPTZ) followed by spectrophotometric detection at 595 nm [*Myklestad et al.*, 1997; *Hung et al.*, 2001]. The system was standardized daily with D-glucose. The precision is ±0.6 μmol C L^{-1} for monosaccharides and ±0.7 μmol C L^{-1} for total saccharides (DCho), and the detection limit was ~2 μmol C L^{-1}. See *Nieto-Cid et al.* [2004] for further details.

3.8. Particulate Organic Carbon and Nitrogen (POC and PON)

[20] Suspended organic matter was collected under low vacuum on precombusted (450°C, 4 hours) 25 mm diameter Whatman GF/F filters of 0.7 μm nominal pore size (POC/PON, 0.5–1.5 L of seawater). All filters were dried overnight and frozen (−20°C) before analysis. Measurements of POC and PON were carried out with a Perkin Elmer 2400 CHN analyzer. An acetanilide standard was used daily. The precision of the method is ±0.3 μmol C L^{-1} and ±0.1 μmol N L^{-1}.

3.9. Particulate Organic Phosphorus (POP)

[21] It was determined by $H_2SO_4/HClO_4$ digestion at 220°C of the particulate material collected from 250–500 mL of seawater on Whatman GF/F filters. The phosphoric acid resultant from the digestion was analyzed with the SFA method for phosphate. The precision is ±0.02 μmol P L^{-1}.

3.10. Particulate Saccharides (PCho)

[22] About 250–500 mL of seawater were filtered and stored as indicated for POC, PON and POP. PCho was determined by the anthrone method [*Ríos et al.*, 1998]. It is based on the quantitative reaction of sugars with anthrone in a strongly acid medium at 90°C, to give an intensely colored compound. The absorption was measured at 625 nm. The system was calibrated daily with D-glucose. The precision of the method is ±0.1 μmol C L^{-1}

3.11. Chlorophyll (Chl)

[23] Between 100 and 200 mL of seawater were filtered through GF/F filters and the filters were immediately frozen (−20°C) until analysis. Chl was determined with a Turner Designs 10000R fluorometer after 90% acetone extraction [*Yentsch and Menzel*, 1963]. The precision is ±0.05 μg L^{-1}.

4. Results and Discussion

4.1. Hydrography of NW Iberian Shelf Waters

[24] Figure 2 identifies the seven hydrographic periods defined by *Nieto-Cid et al.* [2004] during the sampling period, on basis of the meteorological conditions (offshore Ekman transport, continental runoff) and the water column response (salinity and temperature):

4.1.1. Period 1 (15 May to 21 August)

[25] Period 1 is characterized by spring and summer upwelling events separated by short intervals of wind calm, which cause a marked thermal stratification with warm waters in the surface layer and cold and salty Eastern North Atlantic Central Water (ENACW) in the bottom (Figures 3a and 3b). Strong gradients of the chemical variables are observed, with high O_{2C} and low N_T, C_{TC}, TAp, and SiO_4 levels in seasonal thermocline waters and low O_{2C} and high N_T, C_{TC}, TAp and SiO_4 in shelf bottom waters (Figures 3c, 3d, and 4a–4c). Accumulations of DOC, DCho, POC and PCho in the surface layer were observed during the periods of wind calm (Figure 5). Maximum primary production rates in the study area are commonly observed in association with this succession of wind stress/relaxation events: *Arístegui et al.* [2006] have proposed an average value of 2.5 g C m^{-2} d^{-1} during the upwelling season off NW Spain. It contrasted with the low organic matter content of ENACW on the shelf (<60 μM DOC, <5 μM DCho, <2.5 μM POC and <0.5 μM PCho), except that in the bottom nepheloid layer, where POC values >5 μM C were commonly observed.

4.1.2. Period 2 (28 August to 18 September)

[26] Period 2 is characterized by a late summer strong upwelling event, which produced the sudden uplift of the cold, salty, O_{2C} and organic-poor matter and nutrient, C_{TC} and TAp rich ENACW to the surface layer, where temperatures <15°C were recorded.

4.1.3. Period 3 (25 September to 30 October)

[27] Period 3 is characterized by autumn downwelling, forced by the predominant southerly winds and low continental runoff (Figure 2), provoked the entry of warm

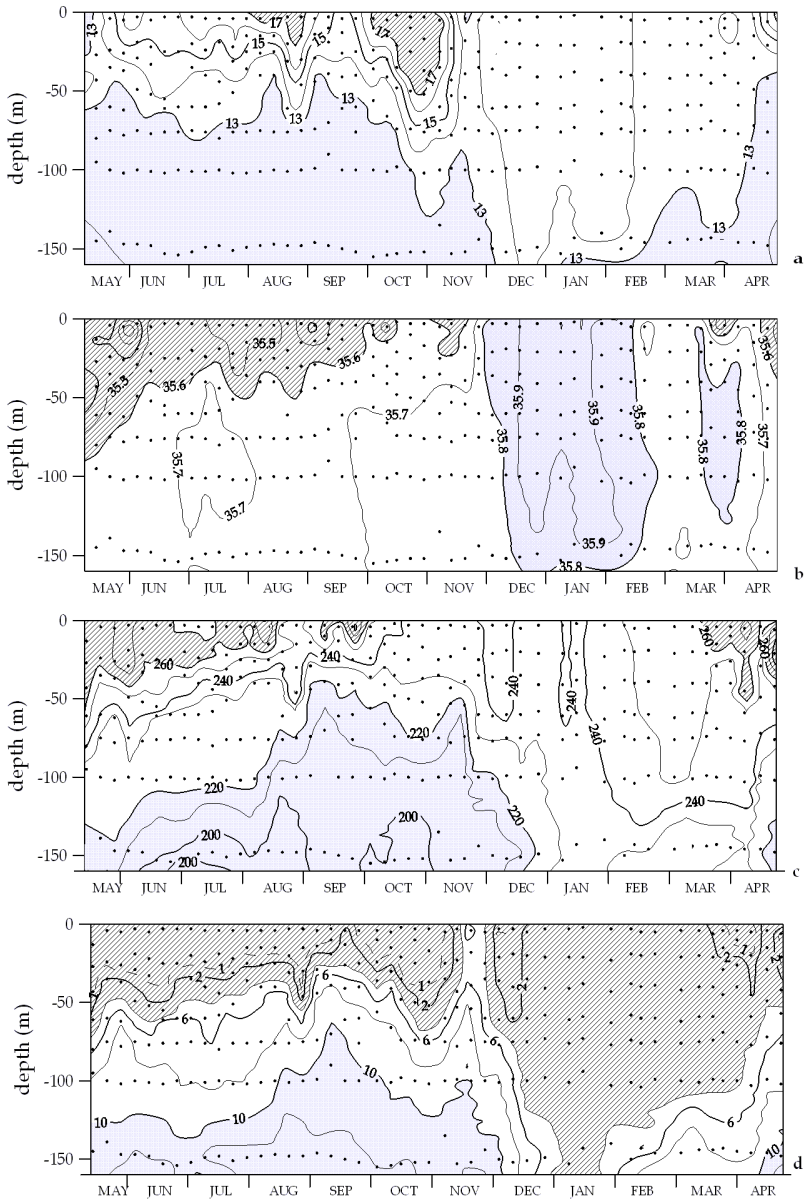

Figure 3. Seasonal evolution of (a) temperature, °C; (b) salinity, practical salinity scale; (c) dissolved oxygen, μmol kg^{-1}; and (d) total inorganic nitrogen, μmol kg^{-1}, at station 03.

(>17°C), O_{2C} and organic-rich matter and nutrient, C_{TC} and TAp poor oceanic surface water.

4.1.4. Period 4 (6–20 November)

[28] Period 4 is the transition from stratification to vertical homogenization enhanced by strong northerly winds (Figure 2).

4.1.5. Period 5 (27 November to 13 February)

[29] Period 5 is the arrival of the Iberian Poleward Current (IPC) carrying warm and salty subtropical surface and central waters (Figures 3a and 3b) to our latitudes, producing a strong impact in the water column: N_T levels remained <1 μM throughout the water column (Figure 3d) and dissolved and particulate organic matter reached minimum levels (Figure 5).

4.1.6. Period 6 (20 February to 26 March)

[30] Period 6 is characterized by winter mixing, the period of maximum vertical homogenization, when ventilation of the water column occurred (Figure 3c) and organic matter levels remained very low (Figure 5) because of the low primary production rates (<0.2 g C m^{-2} d^{-1} [*Álvarez-Salgado et al.*, 2003]).

4.1.7. Period 7 (2–24 April)

[31] Period 7 is characterized by incipient spring stratification under dominant upwelling-favorable winds (Figure 2), which produced a surface accumulation of dissolved and particulate organic materials (Figure 5) in the first spring bloom peak of the season.

[32] Figure 5 shows the seasonal evolution of the DOC, DCho, POC and PCho profiles at the mid shelf station. DON and DOP are significantly correlated with DOC: r = +0.78 for DOC versus DON (n = 284, $p < 0.001$) and r = +0.41 for DOC versus DOP (n = 160, $p < 0.001$). PON and POP also correlate significantly with POC: r = +0.95 for POC versus PON (n = 325, $p < 0.001$) and r = +0.90 for

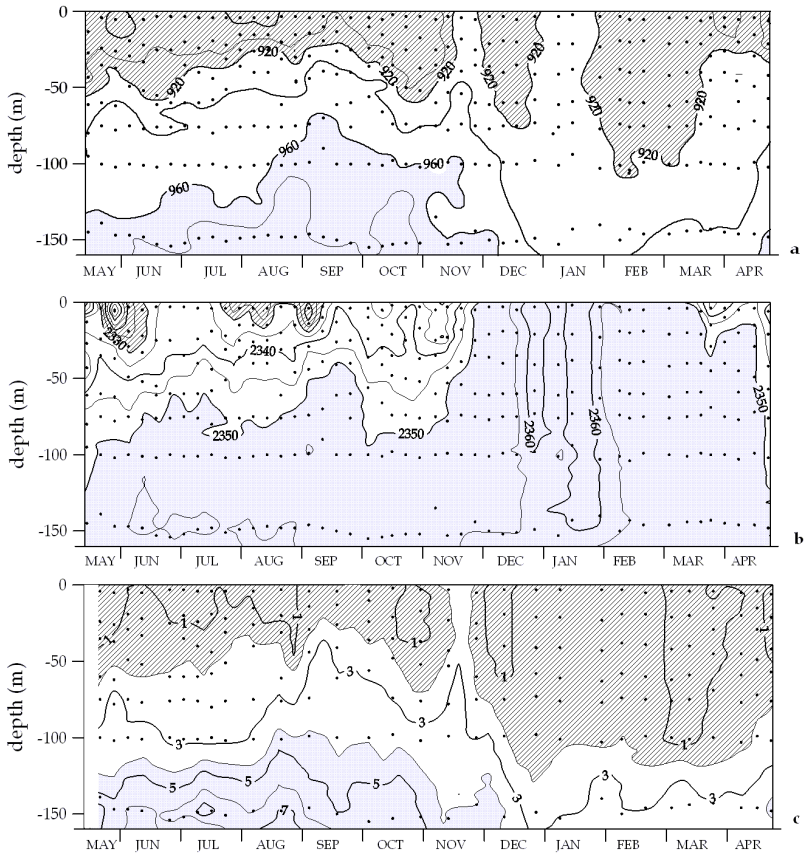

Figure 4. Seasonal evolution of (a) corrected total inorganic carbon, μmol kg^{-1}; (b) potential alkalinity, μeq kg^{-1}; and (c) silicate, μmol kg^{-1}, at station 03.

POC versus POP (n = 213, $p < 0.001$). In addition, DCho correlates with DOC ($r = +0.70$, n = 208, $p < 0.001$) and PCho with POC ($r = +0.87$, n = 215, $p < 0.001$).

[33] Despite the correlations referred above, average profiles of the DOC/DON, POC/PON, DOC/DOP and POC/POP molar ratios (Figures 6a–6d) exhibit a conspicuous vertical structure, characterized by a general increase with depth: the C/N/P ratios of the bottom samples are significantly different for the C/N/P ratios of the surface samples at $p < 0.001$ either for the dissolved or the particulate materials. This is consistent with previous results obtained from marginal seas and open ocean waters [*Williams et al.*, 1980; *Hopkinson et al.*, 1997; *Sanders and Jickells*, 2000; *Hung et al.*, 2003] and can be explained by the preferential oxidation of organic nitrogen and phosphorus compounds at shallower levels in the water column [*Suess and Müller*, 1980; *Shaffer et al.*, 1999]. The elemental C/N/P ratios of DOM are greater than the Redfield ratios, ranging from average C/N values of 12.6 in the surface layer to 14.5 in the bottom layer, and average C/P of 615 in the surface layer to 1090 in the bottom layer. It should be noticed again that the method for the determination of DOP is only able to analyze monophosphoric esters. By contrast, the elemental C/N/P ratios of POM are much closer to the Redfield values: from 6.8 and 100 for C/N and C/P in the surface layer to 9.5 and 140 in the bottom layer.

4.2. Stoichiometry of the Degradation of Biogenic Materials in Coastal and Shelf Waters of NW Spain

[34] Chemical data of waters below the upper mixed layer (AOU > 0) were analyzed along isopycnal surfaces to obtain respiratory ratios. Subsurface waters of the NW Iberian upwelling consists of a mixing of the subtropical and subpolar branches of ENACW with ENACW modified in the surface layer by heat exchange with the atmosphere and continental runoff from the Rías Baixas [*Álvarez-Salgado et al.*, 1997]. Four isopycnal ranges (σ_0) were defined: 26.7–26.8, 26.8–26.9, 26.9–27.0 and 27.0–27.1 (Figure 7a). Samples with $\sigma_0 < 26.7$ were discarded, to minimize the ENACW samples affected by continental runoff/heat exchange with the atmosphere. Therefore for each isopycnal range, a simple two end-member mixing problem has to be solved to obtain an anomaly (ΔY) for each nutrient (Y)

$$\Delta Y = Y - a_0 - a_1 \times T \quad (4)$$

where a_0 and a_1 are the coefficients of the linear regression of Y with temperature. Temperature was chosen as the conservative variable that retains the effect of the two ENACW types mixing because it presents a ratio of the precision of the analytical determination (er) to the standard deviation of the set of field measurements (SD) lower than

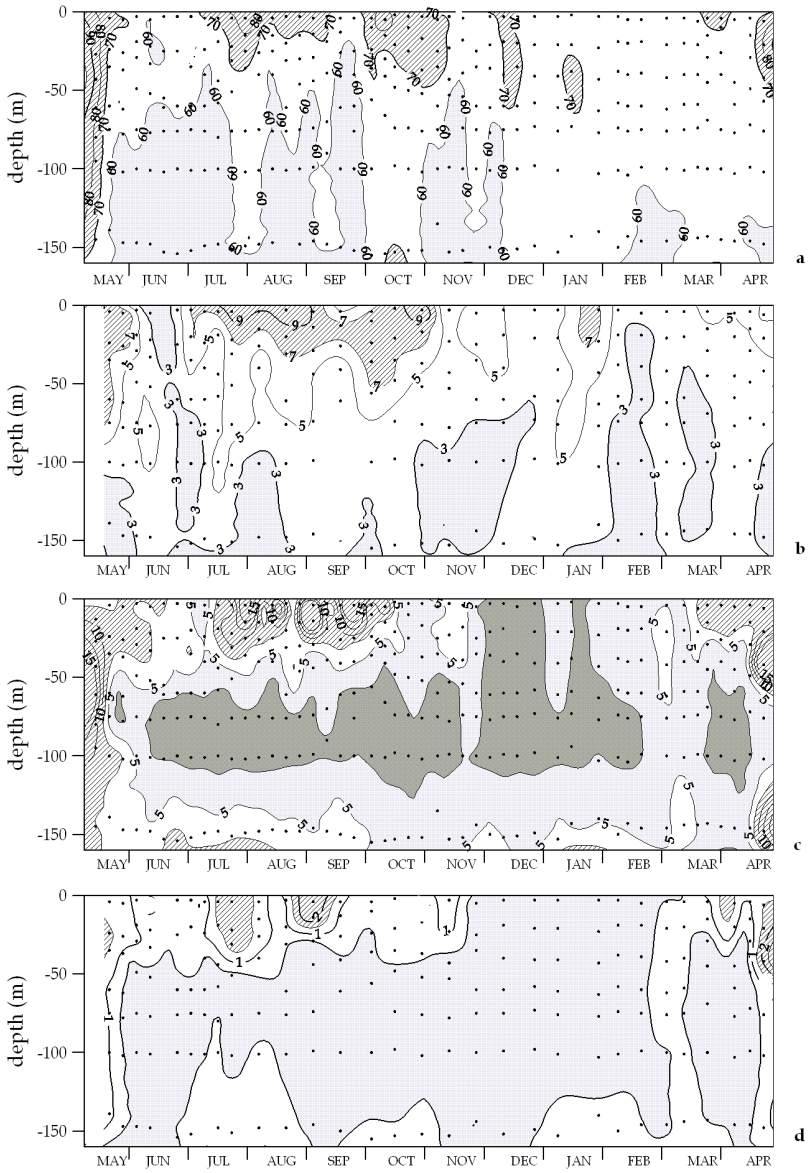

Figure 5. Seasonal evolution of (a) dissolved organic carbon, μmol C L^{-1}; (b) dissolved saccharides, μmol C L^{-1}; (c) particulate organic carbon, μmol C L^{-1}; and (d) particulate saccharides, μmol C L^{-1}, at station 03.

salinity (see equation (6)). ΔY retains only the variability associated to the biogeochemical processes that occur within a given isopycnal range, i.e., the decomposition of organic matter and the dissolution of calcareous and siliceous structures.

[35] Figure 7 also shows a selection of the property versus temperature and property anomaly versus property anomaly plots obtained after applying the isopycnal mixing analysis to the NW Iberian subsurface waters data set. Table 1 summarizes the results obtained analyzing the linear correlation between pair of anomalies of the chemical variables measured during this study for the mid ría (station 00) and mid shelf (station 03) sites. The anomalies obtained for each of the four isopycnal surfaces were analyzed together, to obtain average water column respiratory ratios. The best fit between any pair of nutrient anomalies (ΔX, ΔY) was obtained minimizing the function:

$$\sum_i \left[\left(\Delta X_i - \Delta \hat{X}_i \right)^{w_X} \times \left(\Delta Y_i - \Delta \hat{Y}_i \right)^{w_Y} \right]^2 \qquad (5)$$

where $\Delta\hat{X}$ and $\Delta\hat{Y}$ are the expected values of ΔX and ΔY from the linear regression equation respectively, i.e., $\Delta\hat{Y}_i = m \times \Delta X_i$ and $\Delta\hat{X}_i = \Delta Y_i/m$, with m been the slope of the correlation between ΔX and ΔY; w_X and w_Y are weights for variables X and Y respectively, with w_X, $w_Y \geq 0$ and $w_X + w_Y = 1$. The weight factors were estimated as a function of the precision of the analytical determination of the variable (er) compared with the standard deviation of the set of measurements of that

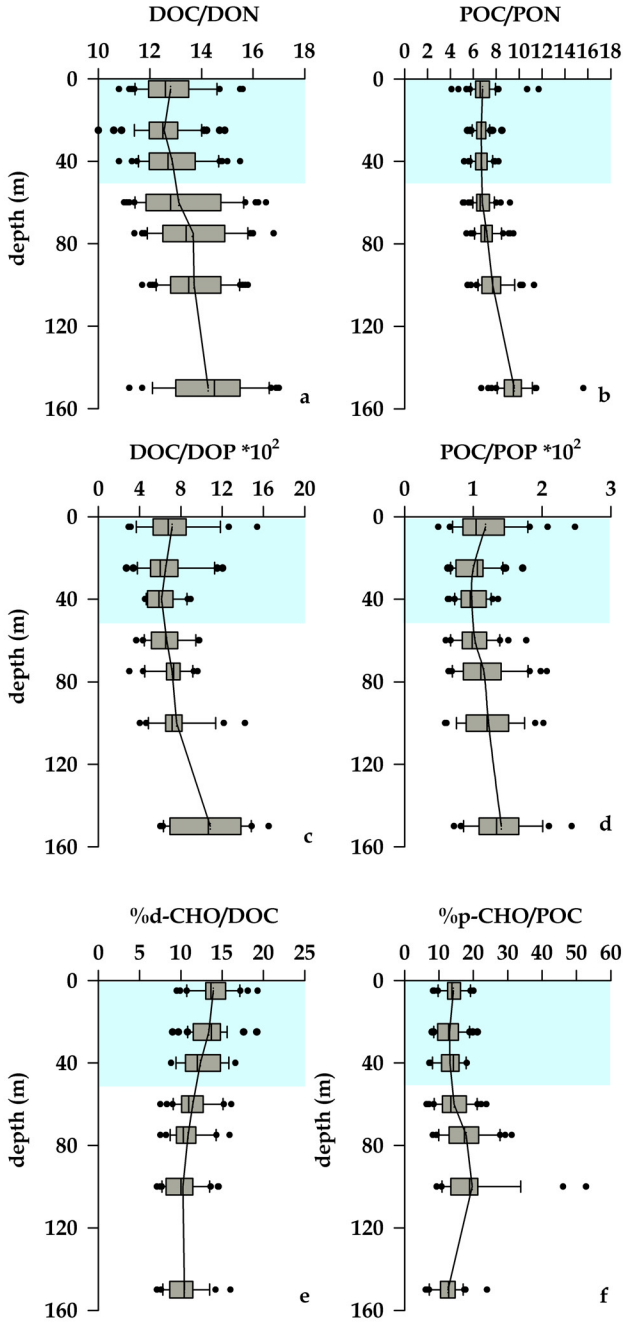

Figure 6. Box whisker plot of molar (a) DOC/DON, (b) POC/PON, (c) DOC/DOP, (d) POC/POP, (e) DCho/DOC, and (f) (PCho/POC)100 ratios. Fifty percent of the data are included within the limit of the boxes, and the caps represent the tenth and ninetieth percentiles. Solid lines represent the average profiles.

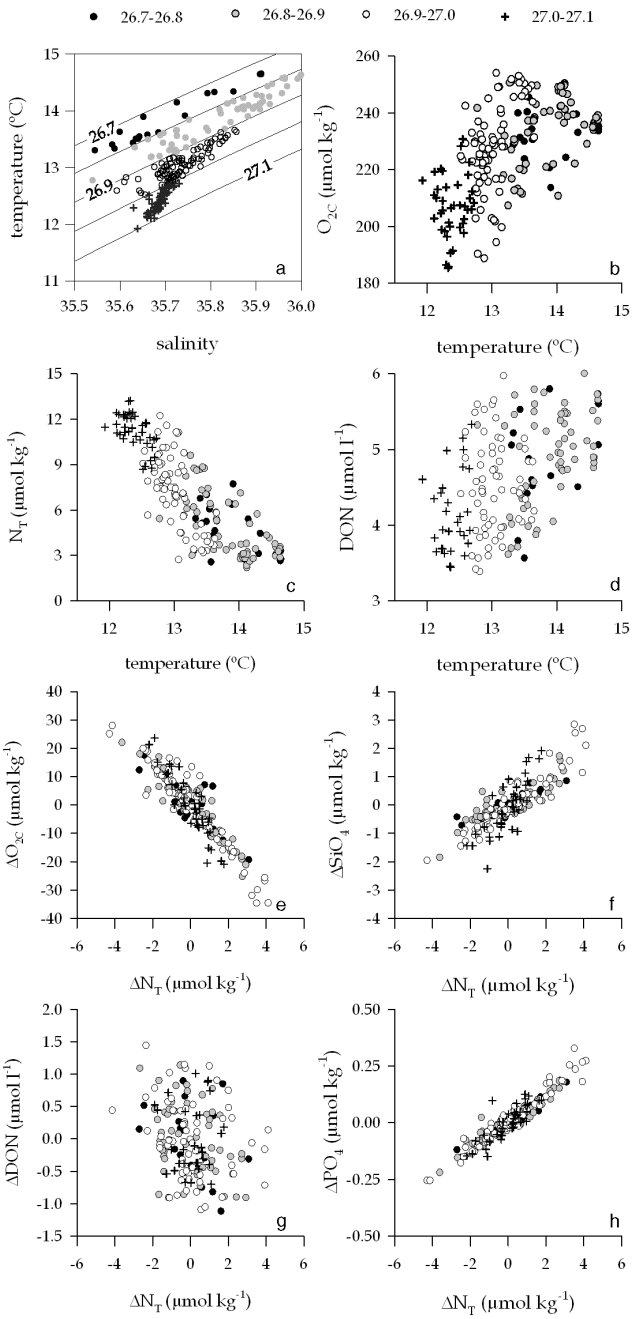

Figure 7. X-Y plot of (a) temperature (in °C) versus salinity, (b) corrected dissolved oxygen (in μmol kg^{-1}) versus temperature (in °C), (c) total inorganic nitrogen (in μmol kg^{-1}) versus temperature (in °C)), (d) dissolved organic nitrogen (in μmol L^{-1}) versus temperature (in °C), (e) corrected dissolved oxygen (in μmol kg^{-1}) versus total inorganic nitrogen (in μmol kg^{-1}) anomalies, (f) silicate (in μmol kg^{-1}) versus total inorganic nitrogen (in μmol kg^{-1}) anomalies, (g) dissolved organic nitrogen (in μmol L^{-1}) versus total inorganic nitrogen (in μmol kg^{-1}) anomalies, and (h) phosphate (in μmol kg^{-1}) versus total inorganic nitrogen (in μmol kg^{-1}) anomalies for the subsurface waters of station 03.

variable for water samples with AOU > 0 (SD). For a given couple of variables X and Y

$$w_X = \left(\frac{er_X}{SD_X}\right) / \left(\frac{er_X}{SD_X} + \frac{er_Y}{SD_Y}\right) \quad (6)$$

Table 1. Regression Coefficient (r), Slope, and Standard Error of the Slope of the Correlation Between Selected Pairs of Nutrient Anomalies for Samples With $\sigma_0 > 26.7$ at Stations 00 and 03[a]

	Station 00			Station 03			
$\Delta Y/\Delta X$	r	Slope	Error	r	Slope	Error	w_X
$\Delta O_{2C}/\Delta C_{TC}$	−0.96	−1.22	±0.05	−0.94	−1.31	±0.03	0.88
$\Delta O_{2C}/\Delta N_T$	−0.90	−10.8	±0.6	−0.92	−8.1	±0.2	0.65
$\Delta O_{2C}/\Delta P$	−0.93	−149	±7	−0.93	−128	±3	0.73
$\Delta N/\Delta SiO_4$	0.90	1.1	±0.1	0.84	1.8	±0.1	0.39
$\Delta SiO_4/\Delta CaCO_3$	0.50	2.5	±0.6	0.48	1.3	±0.2	0.95
$\Delta CaCO_3/\Delta C_{TC}$	0.52	0.05	±0.01	0.46	0.08	±0.01	0.22
$\Delta DOC/\Delta DON$	0.60	6.8	±0.9	0.60	7.9	±0.6	0.66
$\Delta DOC/\Delta DOP$	0.34	120	±22	0.30	151	±16	0.79
$\Delta DCho/\Delta DOC$	0.50	37%	±11%	0.35	28%	±7%	0.19
$\Delta POC/\Delta PON$	0.92	7.4	±0.4	0.93	7.7	±0.2	0.72
$\Delta POC/\Delta POP$	0.71	87	±10	0.90	89	±3	0.84
$\Delta PCho/\Delta POC$	0.54	8%	±2%	0.74	10%	±1%	0.25
$\Delta DOC/\Delta C_{TC}$	−0.33	14%	±5%	−0.17	36%	±15%	0.55
$\Delta DON/\Delta N_T$	−0.41	20%	±6%	−0.25	30%	±9%	0.14
$\Delta DOP/\Delta PO_4$	−0.20	7%	±7%	−0.44	19%	±4%	0.11

[a]The value of w_X, weight for variable X (see equation (6)), is also included. When the notation "%" is used, it means that the slope of the linear regression has been multiplied times 100.

[36] Minimizing equation (5) considering the weight factor of equation (6) ensures that the slopes of the linear regression equations account for the relative precision (er/SD) of the pairs of nutrient anomalies that are correlated each time. The resultant slopes are an intermediate case between (1) a type I regression, which should be applied when $w_X = 0$, $w_Y = 1$ (or $w_X = 1$, $w_Y = 0$) and (2) a type II regression, when $w_X = w_Y = 0.5$ [*Sokal and Rohlf*, 1995]. The slope of a linear regression equation (Y on X) depends strongly on the regression type used: it ranges from a value of $\sum_i(\Delta X_i \times \Delta Y_i)/\sum_i \Delta X_i^2$ for type I to a value of $\sqrt{\sum_i \Delta Y_i^2 / \sum_i \Delta X_i^2}$ for type II. Table 1 summarizes also the values of w_X for the corresponding X/Y pairs.

[37] Especially remarkable in Table 1 are the high correlations found between ΔO_{2C}, ΔC_{TC}, ΔN_T and, ΔP and ΔSiO_4, both in the ría and the shelf waters. The correlations are also significant between the anomalies of the dissolved and the particulate organic materials. These nutrient anomalies can be converted into proportions of saccharides (PCho), lipids (Lip), proteins (Prt), photosynthetic pigments (Chl) and phosphorus compounds (Pho). Table 2 summarizes the average composition of these groups of biomolecules and the relative contribution of each group to the average composition of marine phytoplankton proposed by *Fraga et al.* [1998].

[38] Considering the chemical formulas in Table 2, the following set of five mass balance equations can be written for the particulate organic material:

$$\Delta POC = 138 \times \Delta Prt + 6 \times \Delta PCho + 53 \times \Delta Lip + 45 \times \Delta Pho + 46 \times \Delta Chl \quad (7)$$

$$\Delta POH = 217 \times \Delta Prt + 10 \times \Delta PCho + 89 \times \Delta Lip + 76 \times \Delta Pho + 52 \times \Delta Chl \quad (8)$$

$$\Delta POO = 45 \times \Delta Prt + 5 \times \Delta PCho + 6 \times \Delta Lip + 31 \times \Delta Pho + 5 \times \Delta Chl \quad (9)$$

$$\Delta PON = 39 \times \Delta Prt + 12 \times \Delta Pho + 4 \times \Delta Chl \quad (10)$$

$$\Delta POP = 5 \times \Delta Pho \quad (11)$$

where ΔPOC, ΔPOH, ΔPOO, ΔPON and ΔPOP are the anomalies (equation (4)) of particulate organic carbon, hydrogen, oxygen, nitrogen and phosphorus and ΔPrt, $\Delta PCho$, ΔLip, ΔPho and ΔChl are the anomalies of particulate proteins, saccharides, lipids, phosphorus compounds and pigments, respectively. Since particulate C, N, P, Cho and Chl have been measured, the system can be solved to obtain the average chemical formula and the proportions of the different biomolecules. Unknowns are ΔPOH, ΔPOO, ΔPrt, ΔLip and ΔPho.

[39] The same set of equations can be used for the case of the dissolved organic matter assuming that the DOM that oxidized in the water column is composed of the same biomolecules as the particulate organic matter. This assumption is supported by (1) the similar results of *Hopkinson et al.* [2002] in the Middle Atlantic Bight; (2) the reduced flushing time of shelf waters of the NW Iberian shelf, 1–2 weeks [*Rosón et al.*, 1999]; and (3) the low $\Delta C/\Delta N/\Delta P$ ratios of DOM (Table 1). Another necessary assumption is that $\Delta Chl = 0$ for dissolved organic matter, which is very reasonable since the porphyrin groups of the chlorophylls are among the most resistant biomolecules in nature [*McCarthy et al.*, 1997].

[40] For the case of the dissolved inorganic nutrients, the chemical composition of the oxidized material and the proportions of the different biomolecules are calculated from the O_2, C_T, N_T and HPO_4^{2-} anomalies. Equations describing the oxidation of proteins, saccharides, lipids and phosphorus compounds can be written

$$C_{138}H_{217}O_{45}N_{39}S + 220\ O_2 + 179\ OH^- \longrightarrow \longrightarrow 138\ HCO_3^- + 39\ NO_3^- + SO_4^{2-} + 129\ H_2O \quad (12)$$

$$C_6H_{10}O_5 + 6\ O_2 + 6\ OH^- \longrightarrow 6\ HCO_3^- + 5\ H_2O \quad (13)$$

$$C_{53}H_{89}O_6 + 72.25\ O_2 + 53\ OH^- \longrightarrow 53\ HCO_3^- + 44.5\ H_2O \quad (14)$$

Table 2. Chemical Composition of the Main Organic Products of Synthesis and Early Degradation of Marine Phytoplankton According to *Fraga et al.* [1998][a]

	Chemical Formula	Percentage, w/w
Phosphorus compounds	$C_{45}H_{76}O_{31}N_{12}P_5$	12.1
Pigments	$C_{46}H_{52}O_5N_4Mg$	2.0
Proteins	$C_{138}H_{217}O_{45}N_{39}S$	45.7
Saccharides	$C_6H_{10}O_5$	22.7
Lipids	$C_{53}H_{89}O_6$	17.5
Average composition	$C_{106}H_{171}O_{41}N_{16}P$	100.0

[a]Percentages (in weight (w)) of each group correspond to the average composition of marine phytoplankton.

Table 3. Average Chemical Composition of the Products of Early Degradation of Marine Phytoplankton Photosynthesis as Obtained From Inorganic Nutrients, Dissolved Organic Matter, and Particulate Organic Matter[a]

Nutrients	Station 00	Station 03
	Nutrients	
R_C	1.28–1.45	1.39–1.49
Phosphorus compounds	10.0–13.8	12.7–15.1
Proteins	33.4–46.1	50.4–59.9
Lipids	5.1–35.0	5.1–20.0
Saccharides	51.5–5.0	31.9–5.1
	DOM	
R_C	1.36	1.36
Phosphorus compounds	10.4	8.2
Proteins	44.6	41.1
Lipids	8.8	18.2
Saccharides	36.3	32.4
	POM	
R_C	1.43	1.42
Phosphorus compounds	15.8	14.9
Proteins	41.1	40.8
Lipids	31.6	31.4
Saccharides	11.5	12.9

[a] R_C is in mol O_2 (mol C)$^{-1}$; phosphorus compounds, proteins, lipids, and saccharides are in percent (w/w).

$$C_{45}H_{76}O_{31}N_{12}P_5 + 69.75\ O_2 + 67\ OH^- \longrightarrow \longrightarrow 45\ HCO_3^- + 12\ NO_3^- + 5\ HPO_4^{2-} + 46.5\ H_2O \quad (15)$$

[41] The corresponding linear system of mass balance equations is

$$\Delta O_{2C} = 220 \times \Delta Prt + 6 \times \Delta DCho + 72.25 \times \Delta Lip + 69.75 \times \Delta Pho \quad (16)$$

$$\Delta C_{TC} = -138 \times \Delta Prt - 6 \times \Delta DCho - 53 \times \Delta Lip - 45 \times \Delta Pho \quad (17)$$

$$\Delta N_T = -39 \times \Delta Prt - 12 \times \Delta Pho \quad (18)$$

$$\Delta P = -5 \times \Delta Pho \quad (19)$$

[42] O_{2C} is used in equation (16) because dissolved oxygen consumption in equations (12)–(15) is referred to the oxidation state of nitrate (equation (1)). In addition, since equations (12)–(15) refer only to the oxidation of organic carbon, the influence of the precipitation/dissolution of $CaCO_3$ must be corrected by using C_{TC} (equation (3)) in equation (17). TA_P (equation (2)) also allow us to estimate the dissolution of calcareous structures ($\Delta CaCO_3$):

$$\Delta CaCO_3 = -\frac{1}{2} \times \Delta TA_P \quad (20)$$

[43] Introducing the nutrient ratios of Table 1 in equations (7)–(11) and (16)–(19) it is possible to obtain the average biochemical composition of the organic and inorganic materials mineralized in bottom waters of the ría and the shelf of the NW Iberian upwelling system during a complete seasonal cycle. The R_C ratio ($=-\Delta O_{2C}/\Delta C_{TC}$) cannot be directly used because it is affected by the dissolution of anthropogenic CO_2. Therefore we tested the whole range of possible R_C values. It varies from 1.00 (100% saccharides) to 1.59 (100% proteins). Following *Anderson* [1995], we arbitrarily established that only the R_C values that produce a percentage >5% for saccharides and lipids would be valid. Results are shown in Table 3; it ranges from 1.28 to 1.45 in the ría and from 1.39 to 1.49 in the shelf water. Note that the calculated R_C values are 1.22 and 1.29 for the ría and the shelf, respectively (Table 1), i.e., out of the permitted range. Table 3 also shows the biochemical composition of the materials mineralized as obtained from the inorganic nutrients, the DOM and the POM anomalies. The results presented in Table 3 also allow us to write the following biochemical reactions for the decomposition of the biogenic material:

[44] Mid ría, from nutrients anomalies (using an average $R_C = 1.37$)

$$(C_{108}H_{176}O_{46}N_{14}P)(SiO_2)_{13}(CaCO_3)_5 + 146.5\ O_2 + 57\ H_2O \longrightarrow \longrightarrow 113\ HCO_3^- + 14\ NO_3^- + HPO_4^{2-} + 13\ H_4SiO_4 + 5\ Ca^{2+} + 124\ H^+ \quad (21)$$

[45] Mid ría, from DOM anomalies

$$C_{116}H_{186}O_{55}N_{17}P + 157.5\ O_2 + 33\ H_2O \longrightarrow \longrightarrow 116\ HCO_3^- + 17\ NO_3^- + HPO_4^{2-} + 135\ H^+ \quad (22)$$

[46] Mid ría, from POM anomalies

$$C_{87}H_{141}O_{27}N_{11}P + 123.75\ O_2 + 23.5\ H_2O \longrightarrow \longrightarrow 87\ HCO_3^- + 11\ NO_3^- + HPO_4^{2-} + 100\ H^+ \quad (23)$$

[47] Mid shelf, from nutrients anomalies (using an average $R_C = 1.44$)

$$(C_{91}H_{145}O_{36}N_{16}P)(SiO_2)_9(CaCO_3)_6 + 129\ O_2 + 49\ H_2O \longrightarrow \longrightarrow 97\ HCO_3^- + 16\ NO_3^- + HPO_4^{2-} + 9\ H_4SiO_4 + 6\ Ca^{2+} + 109\ H^+ \quad (24)$$

[48] Mid shelf, from DOM anomalies

$$C_{156}H_{251}O_{65}N_{20}P + 212.5\ O_2 + 42\ H_2O \longrightarrow \longrightarrow 156\ HCO_3^- + 20\ NO_3^- + HPO_4^{2-} + 178\ H^+ \quad (25)$$

[49] Mid shelf, from POM anomalies

$$C_{92}H_{149}O_{29}N_{12}P + 131\ O_2 + 25\ H_2O \longrightarrow \longrightarrow 92\ HCO_3^- + 12\ NO_3^- + HPO_4^{2-} + 106\ H^+ \quad (26)$$

[50] The H^+ produced during the oxidation of biogenic materials is mainly consumed by the carbonic/boric acids buffer system of seawater.

4.2.1. Respiration of Organic Biomolecules

[51] Sinking, particulate and dissolved organic matter has different gravity properties, they cycle differently in the ocean, and they have different elemental ratios [e.g., *Loh and Bauer*, 2000; *Hopkinson et al.*, 1997, 2002]. At station E00, the variation of CO_2 caused by the oxidation of organic matter (C_{TC}) was 25.6 μmol C L^{-1}, whereas the variation of DOC and POC observed at this station was 4.0 and 4.4 μmol C L^{-1}, respectively. This indicates that only 33% (=(4.0 + 4.4)/25.6) of the observed C_{TC} increase can be accounted for by the combined loss of DOC (16%) and POC (17%). Similarly, C_{TC}, DOC and POC variations of 10.0, 3.5 1.8 μmol C L^{-1} were observed at station E03, respectively. This indicates that about 53% (=(3.5 + 1.8)/10.0) of the C_{TC} increase in the water column can be accounted for (35% from DOC and 18% from POC). These observations suggest that 50–70% of the change observed in the water column C_{TC} might have been derived from the oxidation of organic matter, like large fast sinking particles, which could not be captured by our method (representative for particles in the 1–200 μm size range).

[52] Remarkable differences were found between the average composition of the dissolved, particulate and missing sinking organic materials that are mineralized in the waters below the upper mixed layer of the NW Iberian upwelling system. Regarding the dissolved material, there are not differences between the mid ría and mid shelf sites and the most conspicuous characteristic of this material is that saccharides are preferentially consumed (32–36%; Table 3) as compared with a material of Redfield composition (22.7%; Table 2). As for the case of the dissolved material, the composition of the oxidized particulate organic matter did not differ between the ría and the shelf ($p < 0.05$), but in this case lipids are preferentially oxidized: 31% (Table 3) as compared with 17.5% for a material of Redfield composition (Table 2). Finally, assuming average R_C values of 1.37 and 1.44 for the mid ría and mid shelf stations respectively, it results that the missing fraction of mineralized organic material experiences a preferential consumption of saccharides in the mid ría (31% as compared with 22.7% in Table 2) and of proteins in the mid shelf (55% as compared with 46% in Table 2).

[53] *Hopkinson et al.* [2002] were able to differentiate between labile and recalcitrant materials in the mesotrophic Middle Atlantic Bight. The C/N/P ratios of the labile material were similar to the values obtained in the NW Iberian Peninsula and indicate that the stoichiometry of DOM respiration is similar to that for particles [*Garber*, 1984]. The study of *Hopkinson et al.* [2002] showed that DOP was more labile than DON and DON more than DOC. This result was also observed by *Lucea et al.* [2003] in a different environment: the oligotrophic NW Mediterranean. They both confirmed previous conclusions reached by *Jackson and Williams* [1985] and *Hopkinson et al.* [1997] about preferential degradation of phosphorus. *Abell et al.* [2000] merit an special mention since they were able to differentiate the organic matter respiration in upper thermocline waters of the subtropical (oligotrophic) and temperate (mesotrophic) North Pacific Ocean: DOC+POC respiration exhibited a C/N molar ratio of 30 ± 10 in the subtropical and 8 ± 1 in the temperate North Pacific. *Hung et al.* [2003] obtained a C/N molar ratio of DOM respiration of 8.4 and a N/P molar ratio of 19 in the East China Sea, suggesting that they are due to the recently produced fractions. Therefore there is a body of evidence in the literature supporting the fact that the labile dissolved organic material consumed in mesotrophic environments, especially in coastal areas, has a composition similar to the particulate and sinking organic particles.

[54] Since most experimental work on nutrients production from particulate and dissolved organic matter has dealt with laboratory decomposition studies, this work is likely the first estimation in the field of the molecular composition of the mineralized dissolved organic matter in a coastal environment. This type of analysis is more accurate than the estimation of respiration ratios based on the vertical profiles of the bulk C/N/P ratios for DOM and POM as shown in Figure 6, because DOM and POM concentrations can contain refractory components and preformed contributions.

4.2.2. Dissolution of Siliceous and Calcareous Structures

[55] The ratio between soft and hard biogenic material decomposition rates varies with depth in the oceans. Since the upper ocean is $CaCO_3$ over saturated [*Takahashi et al.*, 1981; *Broecker and Peng*, 1982], carbon regeneration at that level is predominantly due to the oxidation of organic carbon [*Honjo et al.*, 1982; *Honjo and Manganini*, 1993]. However, a recent review of the global carbonate budget showed evidences that 60–80% of the biogenic $CaCO_3$ dissolves in the upper 1000 m, above the lysocline, as a result of biological mediation [*Milliman et al.*, 1999]. In deeper layers, the dissolution of hard structures predominates because of the increased pressure, decreased temperature and longer residence times [*Broecker and Peng*, 1982]. These authors, using the GEOSECS data set, estimated a $\Delta CaCO_3/\Delta C_{TC}$ ratio of ~0.1 for the permanent thermocline and ~0.5 for deep waters. *Takahashi et al.* [1985] obtained a $\Delta CaCO_3/\Delta C_{TC}$ ratio of 0.05 for the upper and 0.08 for the lower permanent thermocline of the North Atlantic. Finally, *Ríos et al.* [1995] found a $\Delta CaCO_3/\Delta C_{TC}$ ratio of 0.08 for the upper 2300 m and 0.52 for deeper waters of the eastern North Atlantic Ocean.

[56] A $\Delta CaCO_3/\Delta C_{TC}$ ratio of 0.05 ± 0.01 was estimated for shelf subsurface waters of the NW Iberian upwelling system (Table 1). This value is within the range mentioned for the upper thermocline waters. A higher $\Delta CaCO_3/\Delta C_{TC}$ value of 0.08 ± 0.01 was calculated for the subsurface waters of the Ría de Vigo. The water column below the mixed layer is always supersaturated with respect to calcite and aragonite (average ± SD, 312 ± 42% and 200 ± 28% respectively). Therefore $CaCO_3$ dissolution should occur preferentially at or near the top of sediments [*Archer et al.*, 1989]. The high organic matter content of the sediment, either in the rías [*Vilas et al.*, 2005] or the inner shelf [*Lopez-Jamar et al.*, 1992], creates an environment where the dissolution of $CaCO_3$ is favored by strong acidification. In fact, the sediments inside the rías are characterized by low proportions of $CaCO_3$ where the organic matter content is high [*Vilas et al.*, 2005].

[57] Regarding biogenic silica, it is also exported to the deep ocean as sinking particles, where dissolution occurs. As for the case of $CaCO_3$, most of the silica dissolution takes place below the main thermocline. The high covariation between alkalinity and silicate profiles in open ocean

deep waters [*Brewer et al.*, 1995; *Broecker and Peng*, 1982; *Ríos et al.*, 1995] is probably due to the biologically mediated dissolution of these hard structures in the microenvironments created by marine snow, zooplankton guts, etc. According to *Milliman et al.* [1999] and *Tréguer et al.* [1995], the open ocean $CaCO_3$ and opal decomposition rates in the water column are $47 \cdot 10^{12}$ mol yr^{-1} and $91 \cdot 10^{12}$ mol yr^{-1} respectively. Therefore a mean $\Delta SiO_4/\Delta CaCO_3$ molar decomposition ratio of ~2 can be proposed. For the North Atlantic, an average $\Delta Si/\Delta CaCO_3$ ratio for the whole water column of 1.4 was calculated by *Pérez et al.* [2002]. According to *Berger and Herguera* [1992], a $\Delta SiO_4/\Delta CaCO_3$ ratio of 1.4 is expected for an area with a mean organic carbon flux of 10 mmol m^{-2} d^{-1}, which is in close agreement with their productivity value for the eastern North Atlantic Ocean [*Martin et al.*, 1993]. Lower $\Delta SiO_4/\Delta CaCO_3$ ratios, around 1.05, were measured in sediment traps deployed at the North Atlantic Bloom Experiment (NABE) site below 3100 m [*Newton et al.*, 1994].

[58] In this study, the $\Delta SiO_4/\Delta CaCO_3$ ratio was found to be variable, with a value of 2.5 ± 0.6 in the Ría de Vigo and 1.3 ± 0.2 in the shelf (Table 1). The latter value is in close agreement with that found at the NABE site. As observed in the open ocean [*Berger and Herguera*, 1992], the $\Delta SiO_4/\Delta CaCO_3$ ratio increases from the shelf to the ría as the organic matter flux increases. Along the middle shelf of the NW Iberian Peninsula, *Álvarez-Salgado et al.* [1997] found a large silicate accumulation in bottom waters due to rapid opal dissolution. Opal dissolution was high compared with organic matter decomposition: the $\Delta N_T/\Delta SiO_4$ molar ratio in the ría (1.1 ± 0.1) is about half than in the shelf, (1.8 ± 0.1; Table 1). In this sense, maximum percentages of opal and diatom valve numbers in sediments were recorded in the main channel of the Ría de Vigo [*Prego et al.*, 1995], suggesting a strong downward flux of diatom frustules there.

4.3. Contribution of DOM to Respiration in the NW Iberian Upwelling

[59] A huge effort has been made over the last decade by marine biogeochemist to understand the role played by DOM in carbon, nitrogen and phosphorus cycles in the oceans. Most of this knowledge has been reviewed in a recent book edited by *Hansell and Carlson* [2002].

[60] One of the key questions to answer is the true contribution of DOM to the apparent oxygen utilization of subsurface ocean waters. According to the results of the biogeochemical general circulation model of *Yamanaka and Tajika* [1997], ~70% of the biogenic organic matter exported from the surface (<100 m) to the central (100–500 m) waters of the World Ocean are sinking particles. The remaining ~30% is in the dissolved form. DOM below 1000 m is extremely refractory, confirming that recycling times of this pool range from years to thousands of years [*Hansell and Carlson*, 1998] and that oxygen consumption is almost exclusively due to large sinking particles [*Jahnke*, 1996].

[61] The analysis of the variation of calculated ΔC_{TC}, ΔDOC and ΔPOC values on the previous section yielded that from 16% to 35% of the organic carbon regenerated in bottom waters of the ría and the shelf, respectively, was in the dissolved form. The increase in the offshore direction is consistent with the larger particle fluxes recorded within the rías [*Varela et al.*, 2004] than over the shelf [*Olli et al.*, 2001]. It is also remarkable the low correlation between DOC and C_{TC} anomalies (lower than −0.33), which confirms the general statement that the variability observed in the AOU of the oceans is mainly linked to the flux of large sinking organic particles [*Anderson and Sarmiento*, 1994]. DON/N_T and DOP/PO_4 anomalies reproduced the same pattern observed for DOC/C_{TC}: the contribution of dissolved organic matter to the mineralization of organic nitrogen and phosphorus increased from the ría to the shelf, ranging from 7% to 30%, and the correlation coefficients were also very low, ranging from −0.20 to −0.44. In the continental shelf of Georges Bank, a region of nearly constant upwelling of nutrient rich deep water that can be compared with the NW Iberian shelf, *Hopkinson et al.* [1997] obtained that 19% and 15% of the mineralized N and P that accumulates in deeper water is due to dissolved organic matter respiration. In open ocean waters of the North Pacific, DON contributed from 10% to 25% to the mineralized nitrate in deep waters according to different estimates [*Jackson and Williams*, 1985; *Maita and Yanada*, 1990]. As indicated in the previous section, *Abell et al.* [2000] differentiated the organic matter respiration in upper thermocline waters of the subtropical (oligotrophic) and temperate (mesotrophic) North Pacific Ocean: dissolved+particulate organic carbon contributed 70% to organic mater respiration in the subtropical North Pacific and only 20% in the temperate North Pacific.

5. Conclusions

[62] Four main conclusions can be extracted from this work about the decomposition of biogenic materials in a coastal upwelling system:

[63] 1. More than 50% of the oxygen consumption in shelf subsurface waters is due to the respiration of large, fast sinking organic matter, 17–18% to particulate organic matter and 16–35% to dissolved organic matter.

[64] 2. The products of early degradation of the sinking particulate and dissolved organic matter can be expressed as a linear combination of the main groups of biomolecules: lipids, saccharides, proteins and phosphorus compounds.

[65] 3. Proteins are preferentially oxidized in the sinking organic matter, saccharides in the dissolved organic matter and lipids in the particulate organic matter, as compared with a biogenic material with the reference Redfield composition.

[66] 4. Biogenic opaline silica preferentially dissolved in the middle ría.

[67] **Acknowledgments.** The authors wish to thank the captain and crew of R/V *Mytilus* and the members of the Department of Oceanography of the Instituto de Investigacións Mariñas and the Group of Physical Oceanography of the University of Vigo for their valuable help. Special thanks go to T. Rellán for dissolved oxygen analyses and J. L. Cortijo and S. Piedracoba for the thermohaline and meteorological data. Financial support for this work came from MCYT grant numbers MAR1999–1039–C02–01 and MAR2000–0880–C02–01 and XUGA grant number PGIDT01MAR40201PN. Fellowships of the Spanish MCYT, the I3P CSIC programme, the MCYT grant REN2002-00503/MAR and the Fundación Provigo funded M.N.-C. and S.B. to carry out this work. C.G.C. developed this work with a contract of the Ramon y Cajal programme of the MCYT.

References

Abell, J., S. Emerson, and P. Renaud (2000), Distributions of TOP, TON and TOC in the North Pacific subtropical gyre: Implications for nutrient supply in the surface ocean and remineralisation in the upper thermocline, *J. Mar. Res.*, *58*, 203–222.

Álvarez-Salgado, X. A., and A. E. J. Miller (1998), Simultaneous determination of dissolved organic carbon and total dissolved nitrogen in seawater by high temperature catalytic oxidation: Conditions for precise shipboard measurements, *Mar. Chem.*, *62*, 325–333.

Álvarez-Salgado, X. A., G. Rosón, F. F. Pérez, and Y. Pazos (1993), Hydrographic variability off the Rías Baixas (NW Spain) during the upwelling season, *J. Geophys. Res.*, *98*, 14,447–14,455.

Álvarez-Salgado, X. A., C. G. Castro, F. F. Pérez, and F. Fraga (1997), Nutrient mineralization patterns in shelf water off the western Iberian upwelling, *Cont. Shelf Res.*, *17*, 1247–1270.

Álvarez-Salgado, X. A., J. Gago, B. M. Míguez, M. Gilcoto, and F. F. Pérez (2000), Surface waters of the NW Iberian margin: Upwelling on the shelf versus outwelling of upwelled waters from the Rías Baixas, *Estuarine Coastal Shelf Sci.*, *51*(6), 821–837.

Álvarez-Salgado, X. A., et al. (2003), The Portugal coastal counter current off NW Spain: New insights on its biogeochemical variability, *Prog. Oceanogr.*, *56*, 281–321.

Anderson, L. A. (1995), On the hydrogen and oxygen content of marine phytoplankton, *Deep Sea Res., Part I*, *42*, 1675–1680.

Anderson, L. A., and J. L. Sarmiento (1994), Redfield ratios of remineralization determined by nutrient data analysis, *Global Biogeochem. Cycles*, *8*, 65–80.

Archer, D., S. Emerson, and C. E. Reimers (1989), Dissolution of calcite in deep-sea sediments: PH and O_2 microelectrode results, *Geochim. Cosmochim. Acta*, *53*, 2831–2845.

Arístegui, J., X. A. Álvarez-Salgado, E. D. Barton, F. G. Figueiras, S. Hernández-León, C. Roy, and A. M. P. Santos (2006), Oceanography and fisheries of the Canary Current/Iberian region of the eastern North Atlantic, in *The Sea*, vol. 14, edited by K. H. Brink and A. R. Robinson, chap. 23, pp. 877–931, John Wiley, Hoboken, N. J.

Armstrong, F. A. J., P. M. Williams, and J. D. H. Strickland (1966), Photo-oxidation of organic matter in sea water by ultraviolet radiation, analytical and other applications, *Nature*, *211*, 481–483.

Berger, W. H., and J. C. Herguera (1992), Reading the sedimentary record of the ocean's productivity, in *Primary Productivity and Biogeochemical Cycles in the Sea*, edited by P. G. Falkowski and A. D. Woodhead, pp. X–X, Springer, New York.

Brea, S., X. A. Álvarez-Salgado, M. Álvarez, F. F. Pérez, L. Mémery, H. Mercier, and M. J. Messias (2004), Nutrient mineralization rates and ratios in the eastern South Atlantic, *J. Geophys. Res.*, *109*, C05030, doi:10.1029/2003JC002051.

Brewer, P. G., D. M. Glover, C. Goyet, and D. K. Shafer (1995), The pH of the North Atlantic Ocean: Improvements to the global model for sound absorption in seawater, *J. Geophys. Res.*, *100*, 8761–8776.

Broecker, W. S., and T.-H. Peng (1982), *Tracers in the Sea*, 690 pp., Lamont Doherty Earth Obs., Palisades, N. Y.

Clark, L. L., E. D. Ingall, and R. Benner (1998), Marine phosphorus is selectively remineralized, *Nature*, *393*, 426.

Clayton, T. D., and R. H. Byrne (1993), Spectrophotometric seawater pH measurements: Total hydrogen ion concentration scale concentration scale calibration of m-cresol purple and at-sea results, *Deep Sea Res., Part I*, *40*, 2115–2129.

Copín-Montegut, C., and G. Copín-Montegut (1983), Stoichiometry of carbon, nitrogen, and phosphorus in marine particulate matter, *Deep Sea Res., Part II*, *30*, 31–46.

Fraga, F., and X. A. Álvarez-Salgado (2005), On the variation of alkalinity during the photosynthesis of phytoplankton, *Cienc. Mar.*, *31*, 627–639.

Fraga, F., A. F. Ríos, F. F. Pérez, and F. G. Figueiras (1998), Theoretical limits of oxygen: Carbon and oxygen:nitrogen ratios during photosynthesis and mineralization of organic matter in the sea, *Sci. Mar.*, *62*, 161–168.

Garber, J. H. (1984), Laboratory study of nitrogen and phosphorus remineralization during the decomposition of coastal plankton and seston, *Estuarine Coastal Shelf Sci.*, *18*, 685–702.

Gilcoto, M., X. A. Álvarez-Salgado, and F. F. Pérez (2001), Computing optimum estuarine residual fluxes with a multiparameter inverse method (OERFIM): Application to the Ría de Vigo (NW Spain), *J. Geophys Res.*, *106*, 31,303–31,318.

Gruber, N., K. Keller, and R. M. Key (2000), What story is told by oceanic tracer concentrations?, *Science*, *290*, 455–456.

Hansell, D. A., and C. A. Carlson (1998), Deep-ocean gradients in the concentration of dissolved organic carbon, *Nature*, *395*, 263–266.

Hansell, D., and C. Carlson (Eds.) (2002), *Biogeochemistry of Marine Dissolved Organic Matter*, Elsevier, New York.

Honjo, S., and S. J. Manganini (1993), Annual biogenic particle fluxes to the interior of the North Atlantic Ocean studied at 34°N 21°W, *Deep Sea Res., Part II*, *40*, 587–607.

Honjo, S., S. J. Manganini, and J. J. Cole (1982), Sedimentation of biogenic matter in the deep ocean, *Deep Sea Res., Part I*, *29*, 609–625.

Hopkinson, C. S., B. Fry, and A. M. Nolin (1997), Stoichiometry of dissolved organic matter dynamics on the continental shelf of the northeastern U.S.A., *Cont. Shelf Res.*, *17*, 473–489.

Hopkinson, C. S., Jr., J. J. Vallino, and A. Nolin (2002), Decomposition of dissolved organic matter from the continental margin, *Deep Sea Res., Part II*, *49*, 4461–4478.

Hung, C. C., D. Tang, K. W. Warnken, and P. H. Santschi (2001), Distribution of carbohydrates, including uronic acids, in estuarine waters of Galveston Bay, *Mar. Chem.*, *73*, 305–318.

Hung, J. J., C.-H. Chen, G.-C. Gong, D.-D. Sheu, and F.-H. Shiah (2003), Distributions, stoichiometric patterns and cross-shelf exports of dissolved organic matter in the East China Sea, *Deep Sea Res., Part II*, *50*, 1127–1145.

Jackson, G. A., and P. M. Williams (1985), Importance of dissolved organic nitrogen and phosphorus to biological nutrient cycling, *Deep Sea Res., Part II*, *32*, 223–235.

Jahnke, R. A. (1996), The global ocean flux of particulate organic carbon: Areal distribution and magnitude, *Global Biogeochem. Cycles*, *10*, 71–88.

Li, Y. H., and T. H. Peng (2002), Latitudinal change of remineralization ratios in the oceans and its implication for nutrient cycles, *Global Biogeochem. Cycles*, *16*(4), 1130, doi:10.1029/2001GB001828.

Loh, A. N., and J. E. Bauer (2000), Distribution, partitioning and fluxes of dissolved and particulate organic C, N and P in the eastern North Pacific and Southern Oceans, *Deep Sea Res., Part II*, *47*, 2287–2316.

Lopez-Jamar, E., R. M. Cal, G. Gonzalez, R. B. Hanson, J. Rey, G. Santiago, and K. R. Tenore (1992), Upwelling and outwelling effects on the benthic regime of the continental shelf off Galicia, NW Spain, *J. Mar. Res.*, *50*, 465–488.

Lucea, A., C. M. Duarte, S. Agustí, and M. Sondergaard (2003), Nutrient (N, P and Si) and carbon partitioning in the stratified NW Mediterranean, *J. Sea Res.*, *49*, 157–170.

Lueker, T. J., A. G. Dickson, and C. D. Keeling (2000), Ocean pCO_2 calculated from dissolved inorganic carbon, alkalinity and equations for K_1 and K_2: Validations based on laboratory measurements of CO_2 in gas and seawater at equilibrium, *Mar. Chem.*, *70*, 105–119.

Maita, Y., and M. Yanada (1990), Vertical distribution of total dissolved nitrogen and dissolved organic nitrogen in seawater, *Geochem. J.*, *24*, 245–254.

Martin, J. H., G. A. Knauer, D. M. Karl, and W. W. Broenkow (1987), VERTEX: Carbon cycling in the northeast Pacific, *Deep Sea Res., Part II*, *34*, 267–285.

Martin, J. H., S. E. Fitzwater, R. M. Gordon, C. N. Hunter, and S. J. Tanner (1993), Iron, primary production and carbon-nitrogen flux studies during the JGOFS North Atlantic Bloom Experiment, *Deep Sea Res., Part II*, *40*, 641–653.

McCarthy, M., T. Pratum, J. Hedges, and R. Benner (1997), Chemical composition of dissolved organic nitrogen in the ocean, *Nature*, *390*, 150–154.

Middelburg, J. J., T. Vlug, and F. J. Van der Nat (1993), Organic matter mineralization in marine systems, *Global Planet. Change*, *8*, 47–58.

Milliman, J. D., P. J. Troy, W. M. Bach, A. K. Adams, Y.-H. Li, and F. T. Mackenzie (1999), Biologically mediated dissolution of calcium carbonate above the chemical lysocline?, *Deep Sea Res., Part I*, *46*, 1653–1669.

Minster, J. F., and M. Boulahdid (1987), Redfield ratios along isopycnal surfaces—A complementary study, *Deep Sea Res., Part A*, *34*, 1981–2003.

Myklestad, S. M., E. Skanoy, and S. Hestmann (1997), A sensitive and rapid method for analysis of dissolved mono- and polysaccharides in seawater, *Mar. Chem.*, *56*, 279–286.

Newton, P. P., R. S. Lampitt, T. D. Jickells, P. King, and C. Boutle (1994), Temporal and spatial variability of biogenic particle fluxes during the JGOFS northeast Atlantic process studies at 47°N, 20°W, *Deep Sea Res., Part*, *41*, 1617–1642.

Nieto-Cid, M., X. A. Álvarez-Salgado, S. Brea, and F. F. Pérez (2004), Carbohydrates in a coastal upwelling system (NW Iberian Peninsula), *Mar. Ecol. Prog. Ser.*, *283*, 39–54.

Olli, K., C. Wexels Riser, P. Wassmann, T. Ratlova, E. Arashkevich, and A. Pasternak (2001), Vertical flux of biogenic matter during a Lagrangian study off the NW Spanish continental margin, *Prog. Oceanogr.*, *51*, 443–466.

Pahlow, M., and U. Riebesell (2000), Temporal trends in deep ocean Redfield ratios, *Science*, *287*, 831–833.

Pérez, F. F., and F. Fraga (1987), A precise and rapid analytical procedure for alkalinity determination, *Mar. Chem.*, *21*, 169–182.

Pérez, F. F., M. Álvarez, and A. F. Ríos (2002), Improvements on the back-calculation technique for estimating anthropogenic CO_2, *Deep Sea Res., Part I*, *49*, 859–875.

Prego, R., R. Bao, and R. Howland (1995), The biogeochemical cycling of dissolved silicate in a Galician Ria, *Ophelia*, *42*, 301–318.

Redfield, A. C., B. K. Ketchum, and F. A. Richards (1963), The influence of organisms on the composition of sea-water, in *The Sea*, vol. 2, *The Composition of Sea Water: Comparative and Descriptive Oceanography*, edited by M. N. Hill, pp. 26–77, Wiley-Interscience, Hoboken, N. J.

Richards, F. A. (1965), Anoxic basins and fjord, in *Chemical Oceanography*, vol. 1, edited by J. P. Riley and G. Skirrow, pp. 611–645, Elsevier, New York.

Ríos, A. F., F. Fraga, and F. F. Pérez (1989), Estimation of coefficients for the calculation of "NO", "PO" and "CO", starting from the elemental composition of natural phytoplankton, *Sci. Mar.*, *53*, 779–784.

Ríos, A. F., T. R. Anderson, and F. F. Pérez (1995), The carbonic system distribution and fluxes in the NE Atlantic during Spring 1991, *Prog. Oceanogr.*, *35*, 295–314.

Ríos, A. F., F. Fraga, F. F. Pérez, and F. G. Figueiras (1998), Chemical composition of phytoplankton and particulate organic matter in the Ría de Vigo, *Sci. Mar.*, *62*, 257–271.

Rosón, G., X. A. Álvarez-Salgado, and F. F. Pérez (1999), Carbon cycling in a large coastal embayment, affected by wind-driven upwelling: Short-time-scale variability and spatial differences, *Mar. Ecol. Prog. Ser.*, *176*, 215–230.

Sambrotto, R. N., G. Savidge, C. Robinson, P. Boyd, T. Takahashi, D. M. Karl, C. Langdon, D. Chipman, J. Marra, and L. Codispoti (1993), Elevated consumption of carbon relative to nitrogen in the surface ocean, *Nature*, *363*, 248–250.

Sanders, R., and T. Jickells (2000), Total organic nutrients in Drake Passage, *Deep Sea Res., Part II*, *47*, 997–1014.

Schneider, B., R. Schlitzer, G. Fischer, and E.-M. Nöthing (2003), Depth-dependent elemental compositions of particulate organic matter (POM) in the ocean, *Global Biogeochem. Cycles*, *17*(2), 1032, doi:10.1029/2002GB001871.

Shaffer, G., J. Bendtsen, and O. Ulloa (1999), Fractionation during remineralization of organic matter in the ocean, *Deep Sea Res., Part I*, *46*, 185–204.

Sharp, J. H., et al. (2004), A direct instrument comparison for measurement of total dissolved nitrogen in seawater, *Mar. Chem.*, *84*, 181–193.

Sokal, R. R., and F. J. Rohlf (1995), *Biometry: The Principles and Practice of Statistics in Biological Research*, 3rd ed., 887 pp., W. H. Freeman, New York.

Suess, E., and P. J. Müller (1980), Productivity, sedimentation rate and sedimentary organic matter in the oceans. II. Elemental fractionation, paper presented at *Symposium on the Benthic Boundary Layer*, Cent. Natl. de la Rech. Sci., Marseille, France.

Takahashi, T., W. S. Broecker, and A. E. Brainbridge (1981), The alkalinity and total carbon dioxide concentration in the world ocean, in *Carbon Cycle Modelling*, edited by B. Bolin, *SCOPE*, *16*, 271–286.

Takahashi, T., W. S. Broecker, and S. Langer (1985), Redfield ratio based on chemical data from isopycnal surfaces, *J. Geophys. Res.*, *90*, 6907–6924.

Tréguer, P., D. M. Nelson, A. J. van Bennekom, D. J. DeMaster, A. Laynaert, and B. Quéguiner (1995), The silicate balance in the world ocean: A reestimate, *Science*, *268*, 375–379.

UNESCO (1986), Progress on Oceanographic Tables and Standards 1983–1986, Work and recommendations of the UNESCO/SCOR/ICES/IAPSO Joint Panel, *UNESCO Tech. Pap. Mar. Sci.*, *50*, Mar. Inf. Cent., Div. of Mar. Sci., UNESCO, Paris.

Varela, M., R. Prego, and Y. Pazos (2004), Vertical biogenic particle flux in a western Galician ria (NW Iberian Peninsula), *Mar. Ecol. Prog. Ser.*, *269*, 17–24.

Vilas, F., A. M. Bernabeu, and G. Méndez (2005), Sediment distribution pattern in the Rias Baixas (NW Spain): Main facies and hydrodynamic dependence, *J. Mar. Syst.*, *54*, 261–276.

Walsh, J. J. (1991), Importance of continental margins in the marine biogeochemical cycling of carbon and nitrogen, *Nature*, *350*, 53–55.

Williams, P. M., A. Carlucci, and R. Olson (1980), A deep profile of some biologically important properties in the central North Pacific gyre, *Oceanol. Acta*, *3*, 471–476.

Wollast, R. (1998), Evaluation and comparison of the global carbon cycle in the coastal zone and in the open ocean, in *The Sea*, edited by K. H. Brink and A. R. Robinson, pp. 213–252, John Wiley, Hoboken, N. J.

Yamanaka, Y., and E. Tajika (1997), Role of dissolved organic matter in the marine biogeochemical cycle: Studies using an ocean biogeochemical general circulation model, *Global Biogeochem Cycles*, *11*, 599–612.

Yentsch, C. S., and D. W. Menzel (1963), A method for the determination of phytoplankton chlorophyll and phaeophytin by fluorescence, *Deep Sea Res. Oceanogr. Abstr.*, *10*, 221–231.

X. A. Álvarez-Salgado, S. Brea, C. G. Castro, M. Nieto-Cid, J. Gago, and F. F. Pérez, Consejo Superior de Investigaciones Científicas, Instituto de Investigacións Mariñas, Eduardo Cabello 6, 36208- Vigo, Spain. (xsalgado@iim.csic.es)

M. D. Doval, Xunta de Galicia, Instituto Tecnolóxico de Medio Mariño (INTECMAR), Peirao de Vilaxóan, Vilagarcía de Arousa, Spain.